Re-emergence of a Polar Instability at High Pressure in $KNbO_3$

Mohamad Baker Shoker,[1,*] Sitaram Ramakrishnan,[2,*] Boris Croes,[3] Olivier Cregut,[3] Nicolas Beyer,[3] Kokou D. Dorkenoo,[3] Pierre Rodière,[2] Björn Wehinger,[4] Gaston Garbarino,[4] Mohamed Mezouar,[4] Marine Verseils,[5] Pierre Fertey,[5] Salia Cherifi-Hertel,[3] Pierre Bouvier,[2] and Mael Guennou[1,†]

[1]*University of Luxembourg, Department of physics and materials science, 30 avenue des Hauts-Fourneaux, 4362 Esch-sur-Alzette, Luxembourg*

[2]*Institut Néel CNRS/UGA UPR2940, 25 Rue des Martyrs, 38042 Grenoble, France*

[3]*Université de Strasbourg, CNRS, Institut de Physique et Chimie des Matériaux de Strasbourg, UMR 7504, 67000 Strasbourg, France*

[4]*ESRF—European Synchrotron Radiation Facility, 71 avenue des Martyrs, CS 40220, 38043 Grenoble Cedex 9, France*

[5]*Synchrotron SOLEIL, L'Orme des Merisiers, Départementale 128, 91190 Saint-Aubin, France*

(Received 8 August 2025; accepted 2 January 2026; published 2 February 2026)

Ferroelectric instabilities in perovskites are known to be suppressed by a moderate hydrostatic pressure. The prediction of their re-entrance in a much higher pressure regime is well accepted theoretically, but a conclusive experimental confirmation is still missing. Here, we show its occurrence in a classical but comparatively underlooked ferroelectric perovskite $KNbO_3$. We use single crystal x-ray diffraction, infrared and Raman spectroscopy, and second-harmonic generation to explore the phase transition sequence at high pressures up to 63 GPa. We show that polar cation displacements emerge locally but have to combine with tilts of the oxygen octahedra that are also developing under pressure. This results in a macroscopically centrosymmetric phase with an incommensurate modulation that reflects the tight competition between the polar and tilt instabilities. Soft modes associated with the tilts and the modulation, along with persistent order-disorder signatures, are clearly observed, suggesting that local disorder plays an important role in mediating this competition.

DOI: 10.1103/vwp9-tr7b

Structural instabilities and distortions in perovskite oxides ABO_3 are fundamental to the understanding of their physical and functional properties. They are commonly decomposed in different types based on their symmetry: tilts of the BO_6 octahedra, (anti)polar displacements of the A and B cations, and distortions of octahedra. As part of a general effort to understand these instabilities and their interplay in detail, perovskites have been studied under hydrostatic pressure with the aim of formulating general rules governing the behavior of their instabilities, isolated and in combination. For a long time, notably following pioneering work by Samara *et al.* [1], the common understanding was that those rules were simple: ferroelectric soft modes at the Brillouin zone center should harden under hydrostatic pressure, while soft tilt modes at the zone boundary should soften. Over time, it was realized that the reality is more complex. Tilt instabilities can in fact be either enhanced or suppressed by pressure, as it was revealed experimentally [2] and subsequently rationalized in several papers refining the general rules with a greater attention to the details of energetics and atomistic interactions [3–5]. Polar instabilities were also found to follow Samara's rules at first [6–8]. Whether through a sequence of known phases or, like $PbTiO_3$, through an unexpected and remarkable morphotropic region with monoclinic structures [9,10], all ferroelectric perovskites eventually reach a paraelectric phase at high pressure that seems to be the end of the ferroelectric soft mode. In the early 2000s, these views were revisited and challenged by first-principle calculations [11–13] with the key prediction that the ferroelectric soft phonon mode indeed hardens at first, thereby causing a ferro- to paraelectric transition, but then resoftens in a much higher pressure regime, albeit with a drastic change in the mode eigenvector. This high-pressure polar instability was predicted to be pretty ubiquitous in perovskite oxides with a d^0 B cation, which could lead to the re-entrance of ferroelectricity, to its emergence in nominally paraelectric crystals and other original phenomena.

As the prototypical displacive ferroelectric perovskite with well-documented soft phonon modes at ambient pressure, lead titanate $PbTiO_3$ was the natural contender to check this prediction. Very early on, a combined XRD and Raman spectroscopy study on $PbTiO_3$ at high pressure was reported, claiming evidence for a new high-pressure ferroelectric phase above 50 GPa [14]. However, the

*These authors contributed equally to this work.

†Contact author: mael.guennou@uni.lu

evidence came from powder diffraction alone and could never be confirmed. In a very recent study [15], second-harmonic generation (SHG) was performed and gave no evidence for a breaking of inversion symmetry up to 90 GPa, leading the authors to conclude on the absence of a high-pressure ferroelectric ground state. Other attempts in other candidate systems ($A^{2+}B^{4+}O_3$ compounds such as $SrTiO_3$, $CaTiO_3$, etc.) [16,17] in similar pressure ranges have been equally unsuccessful in providing a conclusive proof of this high-pressure polar instability. This suggests that it might only emerge at much higher pressures where it would have to compete with transition to postperovskite phases [15]—and where experiments are more challenging.

In this Letter, we investigate the high-pressure behavior of potassium niobate $KNbO_3$, a member of the $A^{1+}B^{5+}O_3$ perovskite family whose instabilities at very high pressures have been left comparatively unexplored experimentally. It is known as a dominantly order-disorder type ferroelectric, where some phonon softening is present but incomplete [18]. Its P-T phase diagram up to the paraelectric cubic phase was mapped in detail [8]. The persistence of a Raman signal [8] and diffuse x-ray scattering up to at least 26 GPa [19] indicates that Nb local disorder persists even in the cubic phase, which does not constitute *a priori* a favorable ground when looking for ferroelectric soft modes. Yet we will show that the ferroelectric instability indeed reappears under pressure but has to coexist with the tilt instability that is also favored by pressure.

$KNbO_3$ single crystals grown by the top-seeded solution growth were purchased from SurfaceNet GmbH (Germany) for a series of high-pressure experiments. Experimental details are given in Supplemental Material [20] (see also Refs. [21–24] therein). All results in the low-pressure range across the ferroelectric to paraelectric transition were found essentially consistent with the literature [8] and will not be shown here. High-pressure single-crystal x-ray diffraction at room temperature was carried out at the SOLEIL synchtrotron source (CRISTAL beamline) and at the ESRF (beamlines ID27 [25] and ID15B [26]). At 37 GPa, we observe the appearance of superlattice reflections at commensurate positions $\mathbf{q} = (\frac{1}{2}, \frac{1}{2}, \frac{1}{2})$ (labelled as the R point of the cubic Brillouin zone) as shown in Fig. 1. All diffraction maxima were indexed on an I-centered lattice, and the structure was successfully described by the space group $I4/mcm$ using the CrysalisPro software package [24] and Jana2020 [27]. It corresponds to a structure with antiphase tilts of oxygen octahedra ($a^0a^0c^-$ in Glazer notation [28]). The presence of this phase has not be reported so far in $KNbO_3$, including in a recent powder diffraction study [29], but this occurrence is not surprising. It is very common in perovskites, ferroelectric or not ($SrTiO_3$ [16], $PbTiO_3$ [14], $BaZrO_3$ [30], $EuTiO_3$ [31]), as a result of a pressure-enhanced instability of this tilt mode at the R point [5]. Complementary first-principle calculations of the phonon dispersion (provided in Supplemental Material [20]) confirmed that the tilt phonon mode at the R point becomes more and more unstable under pressure, and further preliminary results confirm the stabilization of this tetragonal phase under pressure [32].

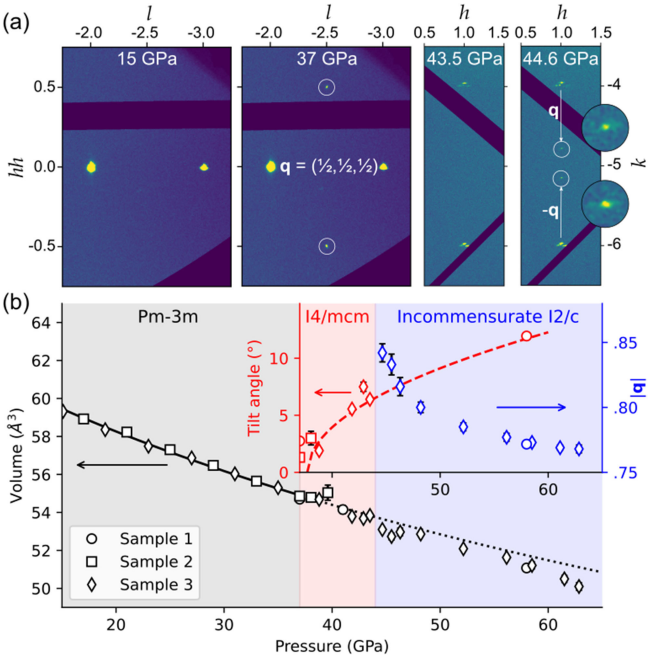

FIG. 1. (a) Reciprocal space reconstructions at selected pressures. Circles indicate the positions of the superlattice reflections, commensurate and incommensurate. The reconstructions at 15 and 37 GPa are in the hhl plane with respect to the cubic lattice and the maps at 43.5 and 44.6 GPa in the $hk\bar{1}$ plane with respect to the tetragonal lattice. (b) Volume, tilt angle, and modulation $|\mathbf{q}|$ as a function of pressure. The solid line is a fit to a second-order Birch-Murnaghan equation of state on the cubic volume, and the dotted line is its extrapolation. The dashed line for the tilt angle is a guide to the eye.

At 44.6 GPa, we observed the reversible emergence of incommensurate satellite reflections at $\mathbf{q} = 0.843(7)\mathbf{b}^*$ [Fig. 1(a)]. The incommensurate $\mathbf{q}$ was observed to shrink rapidly upon increasing pressure and level off at ≈0.77. The superspace approach [33] was employed to elucidate the incommensurate modulation. Initial observation revealed satellites along $\mathbf{a}^*$ and $\mathbf{b}^*$ as shown in Supplemental Material [20]. However, $(3+2)$-dimensional (d) modulation was ruled out in favor of $(3+1)$-d supported by the absence of mixed-order satellites. Instead, the satellites along $\mathbf{a}^*$ belong to another domain brought about by the loss of the fourfold rotational symmetry around $\mathbf{c}^*$. Further evidence proving that the modulated phase is no longer tetragonal arises from the uniaxial direction of the wave vector that is incompatible with the tetragonal ($I4/mcm$) symmetry in $(3+1)$-d but possible with its orthorhombic and monoclinic subgroups [34]. From structural refinements using Jana2020 [27], a better fit was obtained for a monoclinic superspace group $I2/c(0\sigma_1\sigma_2)0s$ [a-unique

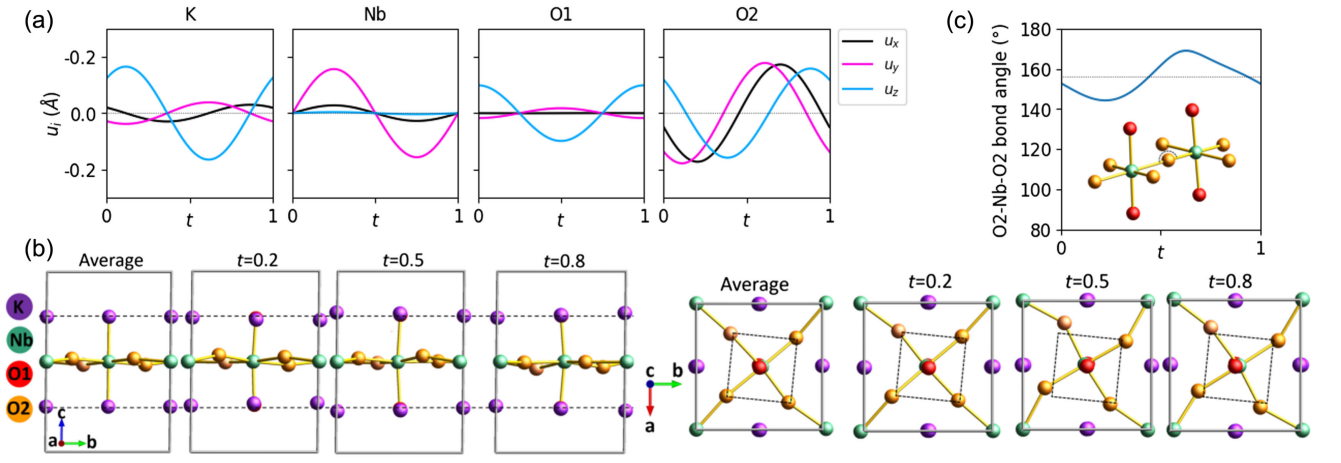

FIG. 2. Atomistic depiction of the modulation at 58 GPa (a) t-plots showing all atomic displacements as a function of the phase of the modulation. (b) Projections of the crystal structure of $KNbO_3$ onto the **bc** and **ab** planes at selected t values. Dashed lines serve as a reference to depict the displacement of the atoms from the average structure. (c) Nb-O-Nb bond angle as a function of t. The dashed horizontal line represents the bond angle for the average structure.

($\sigma_2 = 0$) with $\alpha = 89.40(10)°$] as compared to its orthorhombic supergroup $Ibam(0\sigma 0)s00$. A detailed comparison for both models, as well as other crystallographic information, is provided in Supplemental Material [20].

An atomistic depiction of the modulation at 58 GPa is given in Fig. 2. It is first represented by so-called t plots showing the amplitude of atomic displacements from the average structure as a function of the phase of the modulation t. Figure 2(b) shows a pictorial visualization of the modulation by comparing the average structure to the modulated structure at a few selected t values. In addition, a comprehensive visualization of the modulated structure is provided in the form of a movie generated with Jana2020 [20]. The modulation appears as quite complex and involves a combination of several distortions. Both K and Nb cations are displaced from their high-symmetry position, thereby breaking inversion symmetry locally. However, Nb is displaced longitudinally along **b**, i.e., along the modulation vector, while K (as well as O1) undergo a transverse modulation along **c**. The basal O2 ions appear to be the most heavily modulated in all directions. This can be seen as an *in-phase* tilting motion along the **c** axis that superimposes to the *antiphase* tilting defining the average $I4/mcm$ structure. This results in a significant modulation of the Nb-O2-Nb bond angle between 169.0(3)° and 144.3(4)° [Fig. 2(c)]. Finally, octahedra also undergo stretching along the **c** direction that accompany the K displacements.

It is sometimes argued that conventional XRD cannot unambiguously determine the presence (or breaking) of inversion symmetry and that a dedicated experimental method such as second-harmonic generation (SHG) should be used instead [15]. Indeed, in spite of the use of parameters, like Flack, Parsons, etc., in modern crystallographic softwares that does allow for distinguishing between centrosymmetric and noncentrosymmetric periodic crystals, aperiodic structures can remain problematic. This was illustrated recently with the incommensurate modulation in $EuAl_4$ where the breaking of inversion symmetry was overlooked in a first XRD study [35] before being proposed by SHG measurements [36] and finally corroborated by further diffraction experiments [37]. With this in mind, we performed SHG imaging on a $KNbO_3$ crystal up to 58 GPa. Details are described in Supplemental Material [20] and Refs. [38,39] therein. As shown in Fig. 3, the SHG intensity averaged over the sample area systematically decreases with increasing hydrostatic pressure. Three distinct regimes can be identified, each corresponding to different phases: $Amm2$ (orthorhombic), $P4mm$

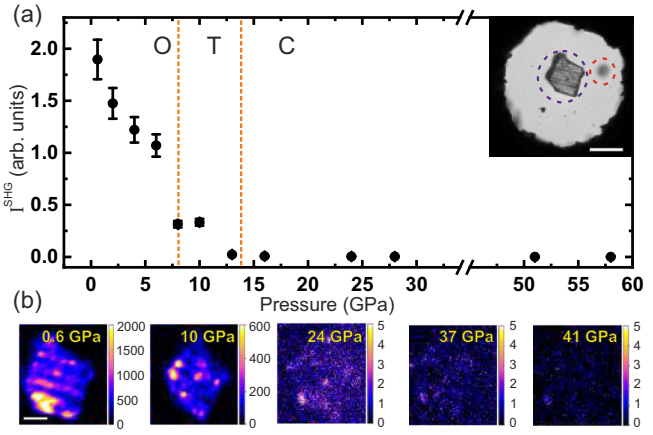

FIG. 3. Variation of the SHG response with pressure. (a) Overall isotropic intensity variation. Dashed lines separate pressure ranges corresponding to the orthorhombic (O), tetragonal (T) and cubic (C) phases. Inset: optical microscopy image showing the sample (blue dashed circle) and the ruby ball (red dashed circle). (b) SHG microscopy images of the sample at selected pressures. The scale bar is 10 μm.

(tetragonal), and ultimately centrosymmetric $Pm\bar{3}m$ (cubic). The corresponding SHG images show a clear domain structure with modulated intensity. At 14 GPa, the intensity drops to essentially zero and does not show any sign of increase up to the maximum pressure of 58 GPa. Importantly, the pressurized sample used for this experiment was the same from which the XRD dataset from Fig. 2 was collected, proving that the incommensurate phase is indeed macroscopically centrosymmetric.

We now turn to the spectroscopic signatures of the transitions. Raman spectroscopy was performed up to a maximum pressure of 58.1 GPa. The transition to the cubic phase was observed at 14.3 GPa. Even though no first-order spectrum is allowed by symmetry in a simple cubic perovskite, the spectrum observed for cubic $KNbO_3$ remains characterized by an intense and structured spectrum shown in Supplemental Material [20]. This is classically explained by the persistence of local disorder; the Nb^{5+} highly charged d^0 cation is known to stay shifted out of the centers of their octahedra through a pseudo-Jahn–Teller distortion, which occurs when the empty d orbitals hydridize with the filled p orbitals of the ligands [40]. Interestingly, this disorder-induced Raman signal weakens but does not vanish with increasing pressure and is still very prominent at 30 GPa at the onset of the antiferrodistortive (AFD) transition. This points to a persistence of this local disorder.

Figure 4(a) shows the Raman spectra across both high-pressure transitions. Between 37 and 43 GPa, we observe several changes that meet the well-documented expectations for the $Pm\bar{3}m$ to $I4/mcm$ AFD transition [16,30]. This includes the emergence of the soft tilt mode [Fig. 4(a)] and the activation of hard modes with $E_g + B_{2g}$ symmetry, the splitting of which is given by symmetry but is negligible in practice [30]. The latter are weak in intensity against the disorder-induced signal, as highlighted in Fig. 4(b), but their positions perfectly match the phonon calculations and their assignment is unambiguous. A much more spectacular change in the Raman signature occurs at 44 GPa with the emergence of the incommensurate modulation. We observe the activation of many sharp hard modes [Fig. 4(a)]. In addition, two modes show a pressure hardening akin to soft-mode behavior. We attribute them to the emergence of specific modes named amplitudon and phason expected from the incommensuration [41]. The detailed mode assignment is beyond the scope of this Letter but we note that the general behavior is compatible with the idea of a change from a phonon density-of-states dominated scattering to a set of discrete lines resulting from the activation of phonons at specific k points. Remarkably, we note that none of the observed soft modes exhibits complete softening, but rather emerges at some finite frequency below which they appear overdamped. This is in line with the behavior of ferroelectric soft modes at ambient pressure and the generally accepted order-disorder character of $KNbO_3$.

Infrared reflectivity (IR) spectra were recorded in the same pressure range on the AILES beamline at the SOLEIL synchrotron source [42]. IR spectroscopy at very high pressures in the phonon energy range, i.e., in the far infrared down to the THz, is intrinsically challenging because of the diffraction limit and the difficulty in focusing a long-wavelength IR beam on a very small sample. As a trade-off, a

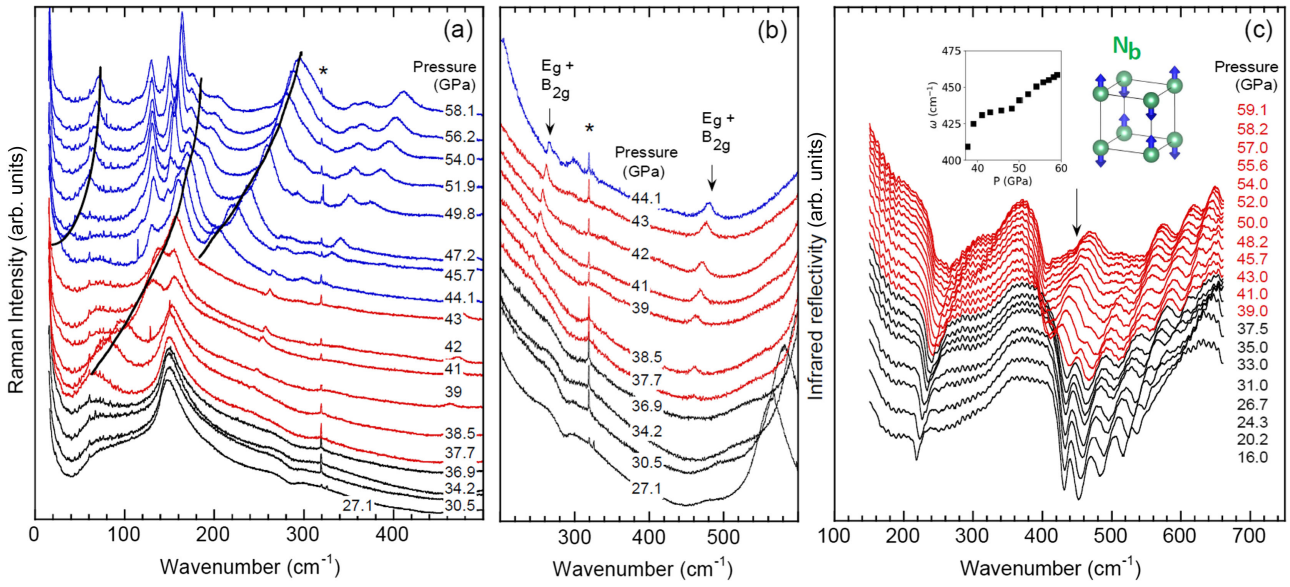

FIG. 4. (a) Low-wavenumber Raman spectra showing the different soft modes as discussed in the text. (b) Raman spectra focused on the emergence of the $E_g + B_{2g}$ hard modes associated with the cubic-to-tetragonal transition. (c) Infrared reflectivity spectra. Inset: frequency of the Nb antipolar mode. Black, red, and blue colors refer to cubic, tetragonal, and incommensurate phases, respectively. The * is an artifact.

100 μm sample was chosen, significantly larger than usual for measurements up to 50 GPa. This allowed us to observe Reststrahlen bands associated with polar phonon modes above 150 cm^{-1} at the cost of nonideal pressure conditions. The spectra are shown in Fig. 4(c). The most prominent signature is the activation of a mode located at about 400 cm^{-1} at 37 GPa. Based on calculated phonon frequencies (provided in Supplemental Material [20]), we attribute this mode to the zone boundary R_4^- mode involving antiparallel motions of Nb. This is known and expected from the symmetry lowering from $Pm\bar{3}m$ to $I4/mcm$ but is usually found to be very weak [43]. We speculate that the unusual strength of this mode here may reflect the proximity of the incommensuration and the modulation of the Nb position. The transition to the incommensurate phase itself was not observed in that experiment, presumably due to the comparatively poorer pressure conditions. Incommensurate phases are known to be fragile: suppression of the modulation due to structural defects like dislocations, stacking faults, or vacancies has been reported in systems such as RTe_3 (R = rare earth) [44] and CuV_2S_4 [45].

Incommensurate modulations in simple perovskites are rare but not unheard of. It was proposed that $EuTiO_3$ shows a modulated structure combining tilts and off-center displacements of Ti along the rotation axis [46,47]. This proposition however was not confirmed by structural refinements, and no such modulation was found under pressure [31]. Much more relevant to the present case are the modulations observed in the model antiferroelectric perovskites $PbZrO_3$ and $PbHfO_3$ under pressure [48,49] and recently fully refined in $PbHfO_3$ as the intermediate phase bridging the paraelectric cubic phase and the $PbZrO_3$-type commensurate antiferroelectric phase [50]. The modulation in $PbHfO_3$ shares some similarities with $KNbO_3$ in that it involves displacements of the A cation as well as additional octahedra tilts. On the other hand, its structure was refined with a higher orthorhombic $Imma(00\gamma)s00$ symmetry, its modulation vector was found to be only weakly temperature dependent, the intermediate $I4/mcm$ commensurate tilted phase was also not present in $PbHfO_3$ and the transition mechanism was discussed as triggered rather than soft-mode driven [49], all of which suggest significant differences in the transition mechanisms.

Generally, incommensurate modulations are understood as the result of a tight competition between two instabilities [41], which here are the polar instability causing the cation off-centering and the zone-boundary instability causing octahedra tilts. The idea of this competition is not new; its basic understanding was substantiated very early on from first principles [51]. However, experimentally, it had led so far to situations where both instabilities are either mutually exclusive, as exemplified by $PbTiO_3$ where the polar instability needs to be killed first by hydrostatic pressure before the tilt instability can develop [10,14], or cause transitions to complex structures by convoluted transition mechanisms like in $PbZrO_3$ [52]. The emergence of a modulated phase in $KNbO_3$ shows that this competition is particularly delicate. Its detailed and quantitative understanding will require further theoretical investigations, but a couple of basic observations can be made. First, $KNbO_3$ has a much larger tolerance factor than $PbTiO_3$ (1.06 vs 1.03), which gives the polar instability a head start under pressure. Besides, it is remarkable that this situation is found in a compound with a significant order-disorder character, while other attempts with more displacive compounds were unsuccessful. This raises the question of whether order-disorder might favor such a coexistence. We also note that the modulation in $KNbO_3$ confirms that it does not depend on the presence of Pb or a cation with a lone electron pair.

In summary, we have shown that $KNbO_3$ exhibits evidence for the re-emergence of a polar instability in the high-pressure regime. Because of a very tight competition with the tilt instability, it does not give rise to a polar phase but to a modulated structure that combines octahedra tilts and off-centering of both A and B cations. Whether this high-pressure polar instability can lead to a ferroelectric phase or to a $PbHfO_3$-like antiferroelectric phase above 63 GPa remains an open question. This calls for an in-depth reinvestigation of the pressure-temperature phase diagram of $KNbO_3$, especially at low temperatures where we might expect an even more intricate competition of ferroelectricity and tilts. The conditions that make this possible in $KNbO_3$, and specifically the possible role of some order-disorder in balancing the competition between instabilities, will also require theoretical investigations with and beyond standard first-principle approaches. Experimental investigations of the local disorder by techniques like x-ray absorption spectroscopies or diffuse scattering are also highly desirable.

Acknowledgments—The authors thank Philippe Ghosez and Hao-Cheng Thong for helpful discussions on preliminary first-principle calculations as well as Jeroen Jacobs for the preparation of the high-pressure cells and Stany Bauchau for technical support at the ESRF beamlines. We acknowledge SOLEIL and the ESRF for provision of synchrotron radiation under Proposals No. 20231689, No. 20241276, and No. HC-6148, respectively. S. R. and P. R. thank the Agence Nationale de la Recherche for support under Project SUPERNICKEL (Grant No. ANR-21-CE30-0041-04). We also acknowledge the Interdisciplinary Thematic Institute 2021-2028 and EUR QMat (No. ANR-17-EURE-0024), as part of the ITI 2021-2028 program supported by the IdEx Unistra (No. ANR-10-IDEX-0002) and SFRI STRAT'US (No. ANR-20-SFRI-0012) through the French Programme d'Investissement d'Avenir.

Data availability—The data that support the findings of this article are openly available [53,54], embargo periods may apply.

[1] G. A. Samara, T. Sakudo, and K. Yoshimitsu, Important generalization concerning the role of competing forces in displacive phase transitions, Phys. Rev. Lett. **35**, 1767 (1975).

[2] P. Bouvier and J. Kreisel, Pressure-induced phase transition in $LaAlO_3$, J. Phys. Condens. Matter **14**, 3981 (2002).

[3] R. J. Angel, J. Zhao, and N. L. Ross, General rules for predicting phase transitions in perovskites due to octahedral tilting, Phys. Rev. Lett. **95**, 025503 (2005).

[4] J. Zhao, N. L. Ross, and R. J. Angel, New view of the high-pressure behaviour of $GdFeO_3$-type perovskites, Acta Crystallogr. Sect. B **60**, 263 (2004).

[5] H. J. Xiang, M. Guennou, J. Íñiguez, J. Kreisel, and L. Bellaiche, Rules and mechanisms governing octahedral tilts in perovskites under pressure, Phys. Rev. B **96**, 054102 (2017).

[6] T. Ishidate, S. Abe, H. Takahashi, and N. Môri, Phase diagram of $BaTiO_3$, Phys. Rev. Lett. **78**, 2397 (1997).

[7] A. Sani, M. Hanfland, and D. Levy, Pressure and temperature dependence of the ferroelectric–paraelectric phase transition in $PbTiO_3$, J. Solid State Chem. **167**, 446 (2002).

[8] P. Pruzan, D. Gourdain, and J. C. Chervin, Vibrational dynamics and phase diagram of $KNbO_3$ up to 30 GPa and from 20 to 500 K, Phase Transitions **80**, 1103 (2007).

[9] Z. Wu and R. E. Cohen, Pressure-induced anomalous phase transitions and colossal enhancement of piezoelectricity in $PbTiO_3$, Phys. Rev. Lett. **95**, 037601 (2005).

[10] M. Ahart, M. Somayazulu, R. E. Cohen, P. Ganesh, P. Dera, H.-K. Mao, R. J. Hemley, Y. Ren, P. Liermann, and Z. Wu, Origin of morphotropic phase boundaries in ferroelectrics, Nature (London) **451**, 545 (2008).

[11] I. A. Kornev, L. Bellaiche, P. Bouvier, P.-E. Janolin, B. Dkhil, and J. Kreisel, Ferroelectricity of perovskites under pressure, Phys. Rev. Lett. **95**, 196804 (2005).

[12] I. A. Kornev and L. Bellaiche, The nature of ferroelectricity under pressure, Phase Transitions **80**, 385 (2007).

[13] E. Bousquet and P. Ghosez, First-principles study of barium titanate under hydrostatic pressure, Phys. Rev. B **74**, 180101 (2006).

[14] P.-E. Janolin, P. Bouvier, J. Kreisel, P. A. Thomas, I. A. Kornev, L. Bellaiche, W. Crichton, M. Hanfland, and B. Dkhil, High-pressure effect on $PbTiO_3$: An investigation by Raman and x-ray scattering up to 63 GPa, Phys. Rev. Lett. **101**, 237601 (2008).

[15] R. E. Cohen, Y. Lin, M. Ahart, and R. J. Hemley, Absence of high-pressure ground-state reentrant ferroelectricity in $PbTiO_3$, Phys. Rev. Lett. **133**, 236801 (2024).

[16] M. Guennou, P. Bouvier, J. Kreisel, and D. Machon, Pressure-temperature phase diagram of $SrTiO_3$ up to 53 GPa, Phys. Rev. B **81**, 054115 (2010).

[17] M. Guennou, P. Bouvier, B. Krikler, J. Kreisel, R. Haumont, and G. Garbarino, High-pressure investigation of $CaTiO_3$ up to 60 GPa using x-ray diffraction and raman spectroscopy, Phys. Rev. B **82**, 134101 (2010).

[18] M. D. Fontana, G. Metrat, J. L. Servoin, and F. Gervais, Infrared spectroscopy in $KNbO_3$ through the successive ferroelectric phase transitions, J. Phys. C **17**, 483 (1984).

[19] S. Ravy, J.-P. Itié, A. Polian, and M. Hanfland, High-pressure study of x-ray diffuse scattering in ferroelectric perovskites, Phys. Rev. Lett. **99**, 117601 (2007).

[20] See Supplemental Material at http://link.aps.org/supplemental/10.1103/vwp9-tr7b for a document containing experimental details, as well as complementary results and tables as detailed in the text, and a movie representing the modulated structure for t values ranging from 0 to 1 in the **bc** and **ab** planes.

[21] G. Shen, Y. Wang, A. Dewaele, C. Wu, D. E. Fratanduono, J. Eggert, S. Klotz, K. F. Dziubek, P. Loubeyre, O. V. Fat'yanov, P. D. Asimow, T. Mashimo, and R. M. M. Wentzcovitch, Toward an international practical pressure scale: A proposal for an IPPS ruby gauge (IPPS-Ruby2020), High Press. Res. **40**, 299 (2020).

[22] K. Takemura, Evaluation of the hydrostaticity of a helium-pressure medium with powder x-ray diffraction techniques, J. Appl. Phys. **89**, 662 (2001).

[23] A. Dewaele and P. Loubeyre, Pressurizing conditions in helium-pressure-transmitting medium, High Press. Res. **27**, 419 (2007).

[24] Rigaku, CrysalisPro Version 171.43.90, Rigaku Oxford Diffraction (2023).

[25] M. Mezouar *et al.*, The high flux nano-x-ray diffraction, fluorescence and imaging beamline ID27 for science under extreme conditions on the ESRF extremely brilliant source, High Press. Res. **44**, 171 (2024).

[26] G. Garbarino, M. E. Hanfland, S. Gallego-Parra, A. D. Rosa, M. Mezouar, D. Duran, K. Martel, E. Papillon, T. Roth, P. Got, and J. Jacobs, Extreme conditions x-ray diffraction and imaging beamline ID15B on the ESRF extremely brilliant source, High Press. Res. **44**, 199 (2024).

[27] V. Petříček, L. Palatinus, J. Plášil, and M. Dušek, Jana2020—A new version of the crystallographic computing system Jana, Z. Kristallogr. **238**, 271 (2023).

[28] A. M. Glazer, Simple ways of determining perovskite structures, Acta Crystallogr. Sect. A **31**, 756 (1975).

[29] Y. Kobayashi, S. Endo, T. Ashida, L. C. Ming, and T. Kikegawa, High-pressure phase above 40 GPa in ferroelectric $KNbO_3$, Phys. Rev. B **61**, 5819 (2000).

[30] C. Toulouse, D. Amoroso, R. Oliva, C. Xin, P. Bouvier, P. Fertey, P. Veber, M. Maglione, P. Ghosez, J. Kreisel, and M. Guennou, Stability of the tetragonal phase of $BaZrO_3$ under high pressure, Phys. Rev. B **106**, 064105 (2022).

[31] D. Bessas, K. Glazyrin, D. S. Ellis, I. Kantor, D. G. Merkel, V. Cerantola, V. Potapkin, S. van Smaalen, A. Q. R. Baron, and R. P. Hermann, Pressure-mediated structural transitions in bulk $EuTiO_3$, Phys. Rev. B **98**, 054105 (2018).

[32] P. Ghosez (private communication).

[33] S. van Smaalen, *Incommensurate Crystallography*, International Union of Crystallography Monographs on Crystallography (Oxford University Press, Oxford, 2007).

[34] H. T. Stokes, B. J. Campbell, and S. van Smaalen, Generation of $(3+d)$-dimensional superspace groups for describing the symmetry of modulated crystalline structures, Acta Crystallogr. Sect. A **67**, 45 (2011).

[35] S. Ramakrishnan, S. R. Kotla, T. Rekis, J.-K. Bao, C. Eisele, L. Noohinejad, M. Tolkiehn, C. Paulmann, B. Singh, R. Verma, B. Bag, R. Kulkarni, A. Thamizhavel, B. Singh, S. Ramakrishnan, and S. van Smaalen, Orthorhombic charge density wave on the tetragonal lattice of $EuAl_4$, IUCrJ **9**, 378 (2022).

[36] F. Z. Yang *et al.*, Incommensurate transverse Peierls transition, arXiv:2410.10539.
[37] S. R. Kotla, L. Noohinejad, P. Pokhriyal, M. Tolkiehn, H. Agarwal, S. Ramakrishnan, and S. van Smaalen, Broken inversion symmetry in the charge density wave phase in $EuAl_4$, Phys. Rev. B **112**, 064113 (2025).
[38] S. Cherifi-Hertel, C. Voulot, U. Acevedo-Salas, Y. Zhang, O. Crégut, K. D. Dorkenoo, and R. Hertel, Shedding light on non-Ising polar domain walls: Insight from second harmonic generation microscopy and polarimetry analysis, J. Appl. Phys. **129**, 081101 (2021).
[39] B. Croes, I. Gaponenko, C. Voulot, O. Crégut, K. D. Dorkenoo, F. Cheynis, S. Curiotto, P. Müller, F. Leroy, K. Cordero-Edwards, P. Paruch, and S. Cherifi-Hertel, Automatic ferroelectric domain pattern recognition based on the analysis of localized nonlinear optical responses assisted by machine learning, Adv. Phys. Res. **2**, 2200037 (2022).
[40] I. Bersuker, On the origin of ferroelectricity in perovskite-type crystals, Phys. Lett. **20**, 589 (1966).
[41] H. Z. Cummins, Experimental studies of structurally incommensurate crystal phases, Phys. Rep. **185**, 211 (1990).
[42] A. Voute, M. Deutsch, A. Kalinko, F. Alabarse, J.-B. Brubach, F. Capitani, M. Chapuis, V. Ta Phuoc, R. Sopracase, and P. Roy, New high-pressure/low-temperature set-up available at the AILES beamline, Vib. Spectrosc. **86**, 17 (2016).
[43] M. Yazdi-Rizi, P. Marsik, B. P. P. Mallett, and C. Bernhard, Anisotropy of infrared-active phonon modes in the monodomain state of tetragonal $SrTiO_3$ (110), Phys. Rev. B **95**, 024105 (2017).
[44] S. Siddique, J. L. Hart, D. Niedzielski, R. Singha, M.-G. Han, S. D. Funni, M. Colletta, M. T. Kiani, N. Schnitzer, N. L. Williams, L. F. Kourkoutis, Y. Zhu, L. M. Schoop, T. A. Arias, and J. J. Cha, Realignment and suppression of charge density waves in the rare-earth tritellurides $R\mathrm{Te}_3$ (R = La, Gd, Er), Phys. Rev. B **110**, 014111 (2024).
[45] S. Ramakrishnan, A. Schönleber, C. B. Hübschle, C. Eisele, A. M. Schaller, T. Rekis, N. H. A. Bui, F. Feulner, S. van Smaalen, B. Bag, S. Ramakrishnan, M. Tolkiehn, and C. Paulmann, Charge density wave and lock-in transitions of CuV_2S_4, Phys. Rev. B **99**, 195140 (2019).
[46] V. Goian, S. Kamba, O. Pacherová, J. Drahokoupil, L. Palatinus, M. Dušek, J. Rohlíček, M. Savinov, F. Laufek, W. Schranz, A. Fuith, M. Kachlík, K. Maca, A. Shkabko, L. Sagarna, A. Weidenkaff, and A. A. Belik, Antiferrodistortive phase transition in $EuTiO_3$, Phys. Rev. B **86**, 054112 (2012).
[47] J.-W. Kim, P. Thompson, S. Brown, P. S. Normile, J. A. Schlueter, A. Shkabko, A. Weidenkaff, and P. J. Ryan, Emergent superstructural dynamic order due to competing antiferroelectric and antiferrodistortive instabilities in bulk $EuTiO_3$, Phys. Rev. Lett. **110**, 027201 (2013).
[48] R. G. Burkovsky, I. Bronwald, D. Andronikova, B. Wehinger, M. Krisch, J. Jacobs, D. Gambetti, K. Roleder, A. Majchrowski, A. V. Filimonov, A. I. Rudskoy, S. B. Vakhrushev, and A. K. Tagantsev, Critical scattering and incommensurate phase transition in antiferroelectric $PbZrO_3$ under pressure, Sci. Rep. **7**, 41512 (2017).
[49] R. G. Burkovsky, I. Bronwald, D. Andronikova, G. Lityagin, J. Piecha, S.-M. Souliou, A. Majchrowski, A. Filimonov, A. Rudskoy, K. Roleder, A. Bosak, and A. Tagantsev, Triggered incommensurate transition in $PbHfO_3$, Phys. Rev. B **100**, 014107 (2019).
[50] A. Bosak, V. Svitlyk, A. Arakcheeva, R. Burkovsky, V. Diadkin, K. Roleder, and D. Chernyshov, Incommensurate crystal structure of $PbHfO_3$, Acta Crystallogr. Sect. B **76**, 7 (2020).
[51] W. Zhong and D. Vanderbilt, Competing structural instabilities in cubic perovskites, Phys. Rev. Lett. **74**, 2587 (1995).
[52] A. K. Tagantsev, K. Vaideeswaran, S. B. Vakhrushev, A. V. Filimonov, R. G. Burkovsky, A. Shaganov, D. Andronikova, A. I. Rudskoy, A. Q. R. Baron, H. Uchiyama, D. Chernyshov, A. Bosak, Z. Ujma, K. Roleder, A. Majchrowski, J.-H. Ko, and N. Setter, The origin of antiferroelectricity in $PbZrO_3$, Nat. Commun. **4**, 2229 (2013).
[53] Dataset for the high-pressure x-ray diffraction data, 10.15151/ESRF-ES-2107750542.
[54] Dataset for the high-pressure FTIR data, 10.5281/zenodo.16780112.